Available free online at www.medjchem.com

Mediterranean Journal of Chemistry

Mediterranean Journal of Chemistry **2024**, 14(2), 122-132

Transition metal (II) complexes of 2-(2,5-dimethoxy-benzylidene)hydrazine-1-carbothioamide: synthesis, characterization and their biological evaluation

Sabiha Sultana [1], Al Akramullazi [1], Md. Faruk Hossen [1], Md. Ali Asraf [1], and Md. Kudrat-E-Zahan [1,*]

[1] Department of Chemistry, Faculty of Science, Rajshahi University, Rajshahi-6205, Bangladesh

Abstract: The current study involved synthesizing Schiff base ligand, 2-(2,5-dimethoxybenzylidene)hydrazine-1-carbothioamide (L) by combining thiosemicarbazide (Th) with 2,5-dimethoxybenzaldehyde (2,5-Dmb), and synthesizing its novel complexes of Co(II), Ni(II), and Cu(II) ions. Elemental analysis, conductance measurements, magnetic susceptibility, molecular weight estimations, FT-IR, ESI-Mass, and UV-Vis spectrum analysis have confirmed the ligand and its metal complexes. The experiment data demonstrated that the ligand binds to the metal atom in a bidentate manner through the N and S atoms. The cytotoxic activity of the synthesized complexes was tested against brine shrimp. All the complexes showed cytotoxic activity; among them, ligands showed a better result with LC_{50} value of 36.93 µg/mL than complexes. Using disc diffusion, the antibacterial action was tested against two Gram-positive bacteria and two Gram-negative bacteria. $[Ni(L)_2]$ was more effective against *E. coli* than the other compounds. The results verified the formation of the novel complexes, and the Ni-complex has the potential to generate novel antibacterial compounds for use in biomedical applications.

Keywords: Schiff base; Metal complex; Cytotoxicity; Antibacterial.

1. Introduction

Carbothioamide is one of the most exciting derivative of thiosemicarbazide. Thiosemicarbazides (Th) have attracted attention since the 1950s for coordinating metal centers and their medicinal and visualization uses [1]. The reaction of Th with aldehydes and ketones results in the formation of molecules known as thiosemicarbazones (Tscs). Over the last several years, these have emerged as the focus of much research because they possess biological activities and pharmacological qualities [2]. Tscs derivatives display a wide range of biological activities, such as antimicrobial, antifungal, antimalarial, antiviral [3], biocidal, anticonvulsant, anti-inflammatory, antileishmanial, antioxidant, antidiabetic [4], anticancer, antitumor, analgesic, anthelmintic [5], herbicidal, antiparasitic [6], antiviral capabilities, and other biological properties that are influenced by the original aldehyde and ketone along with the metal ion [7]. They have shown efficacy as anticonvulsants, insecticides, and fungicides [8]. Tscs have been seeing an increase in attention over the last few years due to their diverse uses in analytical chemistry and industry [9]. They have been thoroughly researched due to their potential uses in catalysis, magnetic characteristics, molecular structures, and materials chemistry [10]. They are utilized as corrosion inhibitors and for removing heavy metals from effluent. They are crucial precursors used to generate bioactive chemicals like beta-lactams [11]. They were utilized for many objectives, including catalytic and enzymatic activities, electronics, cosmetics, polymer industries, luminescent materials, magnetism, and molecular design [12].

Tsc or S-benzyldithiocarbazate molecules may quickly generate strong bonds with transition metals, creating an extended p-conjugated system by deprotonation [13]. According to research, metal complexes of Schiff bases formed from Tscs frequently exhibit more potent and specific biological properties than the equivalent free Tscs [14]. Their complexes are extensively researched due to their intriguing and significant features, particularly their capacity to reversibly bind oxygen in redox systems within living things and facilitate the oxidation of DNA [15]. The creation of C-C bonds, oxidation processes, and many more fascinating chemical reactions can be catalyzed by homogeneous catalysts, which are soluble complexes of transition metals [16]. With their usage in metals analysis, these devices have found utility in optical processing, storing, data processing, and telecommunications infrastructure [17]. Organotin (IV) complexes are intensively researched because of their coordination shapes, structural variety, and strong effects from the molecule's shape and the tin atom's coordination number. Recently,

**Corresponding author: Md. Kudrat-E-Zahan*
Email address: kudrat.chem@ru.ac.bd
DOI: http://dx.doi.org/10.13171/mjc02407261780zahan

Received April 21, 2024
Accepted June 26, 2024
Published July 26, 2024

studies on (E)-2-(2, 5-dimethoxybenzylidene) hydrazinecarbothioamide and its dimers attracted our research interest [18]. Our research aimed to synthesize novel Schiff base metal complexes, characterize them, and evaluate their biological activity.

2. Experimental

2.1. Materials and Reagents

All the chemicals utilized in this investigation were acquired from Aldrich. These included Th, 2,5-dimethoxybenzaldehyde, $Co(CH_3COO)_2.4H_2O$, $Cu(CH_3COO)_2.H_2O$, $Ni(CH_3COO)_2.4H_2O$, Mol. Wt. 248.85; absolute ethanol and methanol that were employed. We did not purify any compounds before using them because they were all analytical grade [19].

Table 1. Lists the specifications of the reagents used

Name of the chemicals	Molecular formula	Formula weight $gmol^{-1}$	Suppliers	Purity
Thiosemicarbazide	CH_5N_3S	91.13	Aldrich	99%
2,5-dimethoxybenzaldehyde	$C_9H_{10}O_3$	166.17	Aldrich	98%
Nickel (II) Acetate Tetrahydrate	$C_4H_{14}NiO_8$	248.84	Aldrich	98%
Copper (II) Acetate Monohydrate	$C_4H_8CuO_5$	198.966	Aldrich	99%
Cobalt (II) Acetate Tetrahydrate	$C_4H_{14}CoO_8$	249.08	Aldrich	97%
Absolute Ethanol	C_2H_5OH	46.07	Crew & Co. (Bd)	99%
Methanol	CH_3OH	32.04	Aldrich	99%
Dimethyl sulfoxide (DMSO)	$(CH_3)_2SO$	78.13	Aldrich	99%

2.2. Physical measurements

The substances' melting points were determined using an Electrothermal 9300. All complexes' molar conductivities were measured using a Cond 7110 WTW conductometer. A solution of KCl was used to calibrate the conductivity cell. The conductivity tests were performed using 5 mM solutions in deionized water that were utilized fresh [20]. A magnetic susceptibility balance was used to determine the moments of magnetism (Matthews Johnson). Running samples as pellets of KBr allowed for the measurement of infrared spectra in the 400-4000 cm^{-1} range using a 9800 FTIR spectrometer (Perkin-Elmer). The electronic spectra of the produced substances were measured employing a Cary Varian UV-Visible spectrometer in the wavelength range of 200-800 nm, with DMSO as the solvent [21]. The carbon, hydrogen, and nitrogen elements were analyzed using a Perkin–Elmer 240C elemental apparatus. ESI-Mass spectra were done with an Agilent Technologies MSD SL Trap mass spectrometer with ESI source coupled with an 1100 Series HPLC system.

2.3. Synthesis of Schiff Base Ligand 2-(2,5-dimethoxybenzylidene)hydrazine-1-carbothioamide ($C_{10}H_{13}N_3O_2S$) (L)

A condensation process between 2,5-Dmb and Th synthesizes the Schiff base ligand, L. An ethanolic solution of 2,5-Dmb (1.66g, 10mmol) was gradually added to a constantly stirred Th (0.911g, 10mmol) solution. This mixture was refluxed for 4-5 hours. Cooling produced an off-white material that was filtered, washed with diethyl ether, and vacuum-dried over anhydrous $CaCl_2$. Thin-layer chromatography (TLC) using n-hexane and chloroform solvents was used to monitor reaction progress and purity. It was off-white and soluble in methanol, ethanol, chloroform, and DMSO, yielding 90%.

Molecular formula: $C_{10}H_{13}N_3O_2S$; Appearance: White; Yield: 79%; Melting point: 231°C; FT-IR (KBr pellet): ν(-OH)-3400 cm^{-1}, ν(>C=O)-1668 cm^{-1}, ν(>C=N)-1596 cm^{-1}; UV/Vis.(DMSO): λ_{max} at 267 nm and 324 nm; Ana. Cal. (Found): C-50.10 (50.15), H-5.47 (5.43), N-17.59 (17.55), S-13.33 (13.37).

2.4. General procedure for the Synthesis of the metal complexes

During the complex formation process, a 15 mL of ethanolic solution containing Cu(II) acetate monohydrate (0.100g, 0.5 mmol), Co(II) acetate tetrahydrate (0.124g, 0.5 mmol), or Ni(II) acetate tetrahydrate (0.124g, 0.5 mmol) was introduced into a two-necked round-bottom flask and subjected to magnetic stirring. A solution containing the Schiff base ligand (0.239g, 1 mmol) in ethanol (20 mL) was slowly added to a reaction mixture while stirred continuously on a magnetic stirrer for 3-4 hours. After

the process of cooling, a solid product with a distinct color was obtained, i.e., the $[Ni(L)_2]$ was dark brown, the $[Cu(L)_2]$ was red, and the $[Co(L)_2]$ was brown. These solids were next subjected to a series of purification steps, including washing with hot ethanol and diethyl ether. The solid was dried using a vacuum desiccator containing anhydrous calcium chloride. The advancement of the reaction was observed by employing thin-layer chromatography (TLC) with n-hexane and chloroform as the chosen solvents. The complexes demonstrated solubility in various solvents, including DMSO. Figure 1 illustrates the chemical structure of the Schiff base under investigation and the typical structure observed in metal complexes.

$[Ni(L)_2]$: Appearance: Dark Brown; Yield: 68%; Melting point: 240°C; Molecular formula: $NiC_{20}H_{24}N_6O_4S_2$; Conductivity: 4 Sm^2mol^{-1}; μ_{eff} B.M: diamagnetic; FT-IR (KBr pellet): ν(-OH)-3393 cm^{-1}, ν(C–O)-1302 cm^{-1}, ν(>C=N)-1575 cm^{-1}, ν(Ni–O)-640 cm^{-1}, ν(Ni–N)-476 cm^{-1}; UV/Vis.(DMSO): λ_{max} at: 300 nm, 366 nm and 400 nm; Ana. Cal. (Found): C-44.79 (44.84), H-4.44 (4.48), N-15.74 (15.69), S-11.99 (11.96), Ni-11.01 (10.97).

$[Co(L)_2]$: Appearance: Dark Brown; Yield: 71%; Melting point: >300°C; Molecular formula: $CoC_{20}H_{24}N_6O_4S_2$; Conductivity: 7 Sm^2mol^{-1}; μ_{eff} B.M: 3.87; FT-IR (KBr pellet): ν(-OH)-3432 cm^{-1}, ν(C–O)-1299 cm^{-1}, ν(>C=N)-1577 cm^{-1}, ν(Co–O)-637 cm^{-1}, ν(Co–N)-481 cm^{-1}; UV/Vis.(DMSO): λ_{max} at: 278 nm and 364 nm; Ana. Cal. (Found): C-44.87 (44.82), H-4.43 (4.48), N-15.64 (15.69), S-11.91 (11.95), Co-11.05 (11.00).

$[Cu(L)_2]$: Appearance: Light Yellow; Yield: 62%; Melting point: >300°C; Molecular formula: $CuC_{20}H_{24}N_6O_4S_2$; Conductivity: 8 Sm^2mol^{-1}; μ_{eff} B.M: 1.74; FT-IR (KBr pellet): ν(-OH)-3424 cm^{-1}, ν(C–O)-1305 cm^{-1}, ν(>C=N)-1577 cm^{-1}, ν(Cu–O)-638 cm^{-1}, ν(Cu–N)-458 cm^{-1}; UV/Vis.(DMSO): λ_{max} at: 262 nm, 290 nm and 418 nm; Ana. Cal. (Found): C-44.40 (44.44), H-4.49 (4.44), N-15.49 (15.55), S-11.82 (11.85), Cu-11.73 (11.77).

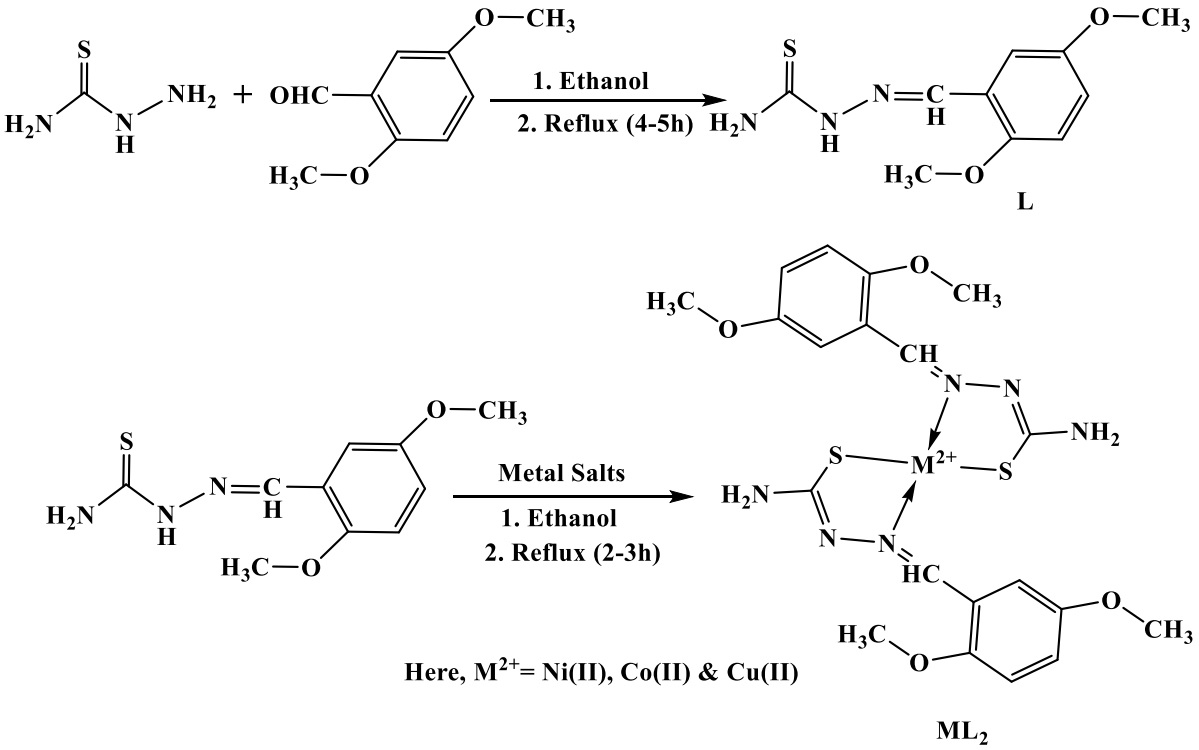

Figure 1. Schematic route for the Synthesis of the ligand and its metal complexes

3. Results and Discussion

3.1. Investigation of Elemental, Physical, and Molar Conductivity

Determining the melting point provides a rough indication of the characteristics of the complexes. Elect electrothermal melting point equipment determined the melting or decomposition temperatures of all the produced ligands and metal complexes. Following the method described in the literature, the metal percentage was determined by complexometric titration with EDTA [22]. Table 1 displays ligands and complexes' physical, elemental, and analytical conductivity statistics.

Table 2. Elements and physical characteristics of Schiff bases and $[Ni(L)_2]$, $[Cu(L)_2]$, $[Co(L)_2]$ complexes.

Compound	Empirical formula	Melting Point(°C)	Color	Λ^a (Sm^2 mol^{-1})	(%) Found (Ana. Cal.)				
					C	H	N	S	M
L	$C_{10}H_{13}N_3O_2S$	233	White	----	50.10 (50.15)	5.47 (5.43)	17.59 (17.55)	13.33 (13.37)	----
$[Ni(L)_2]$	$NiC_{20}H_{24}N_6O_4S_2$	240	Dark Brown	4	44.79 (44.84)	4.44 (4.48)	15.74 (15.69)	11.99 (11.96)	11.01 (10.97)
$[Co(L)_2]$	$CoC_{20}H_{24}N_6O_4S_2$	>300	Dark Brown	8	44.87 (44.82)	4.43 (4.48)	15.64 (15.69)	11.91 (11.95)	11.05 (11.00)
$[Cu(L)_2]$	$CuC_{20}H_{24}N_6O_4S_2$	>300	Light Yellow	7	44.40 (44.44)	4.49 (4.44)	15.49 (15.55)	11.82 (11.85)	11.73 (11.77)

3.2. FT-IR Spectra

A representation of the spectra of Schiff base L, $[Ni(L)_2]$, $[Co(L)_2]$, and $[Cu(L)_2]$ may be found in Figure 2. Spectra like these were acquired by applying the Fourier transform infrared (FT-IR) technology.

The absorption spectrum recorded at wavenumbers of 3431 cm^{-1}, 3177 cm^{-1}, and 3016 cm^{-1} were assigned to the stretching frequencies of the ν(-NH_2), ν(-NH), and ν(-CH) groups, respectively. The spectrum also shows peaks at 1597 cm^{-1} and 1082 cm^{-1}, which can be attributed to the vibrational modes of the ν(C=N) and ν(C=S) functional groups, respectively [23, 24].

The FT-IR spectra of metal complexes show a displacement in the position of the ligand band at 1597 cm^{-1} due to the presence of the azomethine group (>C=N). The shift is observed at 1629 cm^{-1}, 1625 cm^{-1}, and 1619 cm^{-1} for $[Ni(L)_2]$, $[Cu(L)_2]$, and $[Co(L)_2]$ respectively [25]. This change signifies that the metal complexes are bound to metal ions. The ligand's stretching frequency, which surpasses the ν(C=S) stretching frequency, was altered to 1116 cm^{-1}, 1124 cm^{-1}, and 1138 cm^{-1} in the complex spectra for $[Ni(L)_2]$, $[Cu(L)_2]$, and $[Co(L)_2]$ respectively. This finding illustrates the function of Sulphur in the coordinating process. A novel bond elongation frequency was observed at 619 cm^{-1}, 603 cm^{-1}, and 602 cm^{-1}. These frequencies indicate the formation of Ni-S bonds, Cu-S bonds, and Co-S bonds, respectively. A unique bond stretching frequency at 465 cm^{-1}, 459 cm^{-1}, and 463 cm^{-1} indicates the formation of Ni-N, Cu-N, and Co-N bonds, respectively. This fact is crucial to examine. The large peak in $[Ni(L)_2]$, $[Cu(L)_2]$, and $[Co(L)_2]$ complex IR spectra at 3350 to 3450 cm^{-1} was likely caused by moisture in the KBr pellet [26].

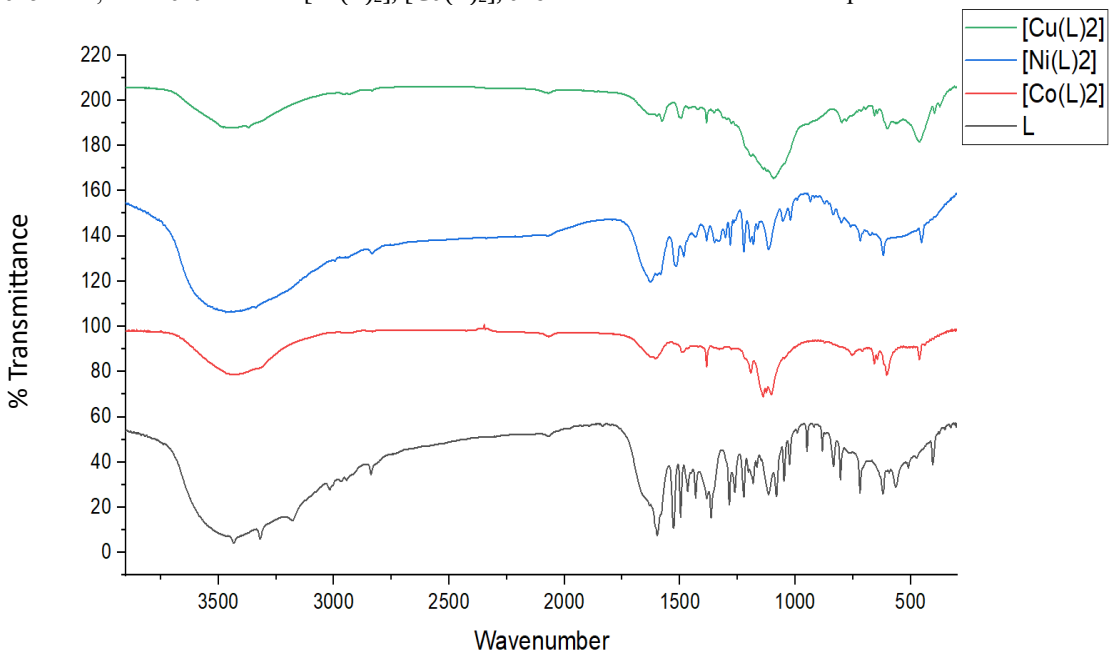

Figure 2. FTIR spectra of L & its metal complexes

3.3. UV-Vis Spectra

Electronic spectroscopy in DMSO was used to analyze the L and its $[Ni(L)_2]$, $[Cu(L)_2]$, $[Co(L)_2]$ complexes from 200 to 800 nm. Table 3 shows the findings. L and its complexes had high visible and ultraviolet absorption bands.

Table 3. The L and $[Ni(L)_2]$, $[Cu(L)_2]$, $[Co(L)_2]$ complexes FTIR spectrum data (in cm^{-1}).

Compounds	ν(-NH_2)	ν(>C=N)	ν(C=S)	ν(C−S)	ν(M−S)	ν(M−N)
L	3431	1597	1082	----	----	----
$[Ni(L)_2]$	3436	1629	----	1116	619	465
$[Cu(L)_2]$	3435	1625	----	1124	603	459
$[Co(L)_2]$	3432	1619	----	1138	602	463

As the L dissolved in DMSO at ambient temperature, its electronic spectra and those of all complexes were recorded. L electronic spectrum shows a high-intensity absorption peak at 311 and 352 nm. The peaks in Figure 3 are attributed to the π→π* and n →π* transitions, respectively [27].

Figure 3 shows three UV-Vis absorption bands for $[Ni(L)_2]$ at 268, 321, and 370 nm. In the $[Ni(L)_2]$, the ligand's electronic spectra changed at 311 and 352 nm. L binding to Ni (II) ions was shown. Peaks at 268 and 321 nm were attributed to the π→π* and n→π* transitions, respectively. Due to an azomethine nitrogen's lone electron pair and antibonding p orbital, these transitions occur. Figure 3 shows ligand-to-metal charge transfer in the compound's 370 nm absorption region. Based on the magnetic moment value and UV spectral data, the [Ni(L)2] may have a square-planar structure [Figure 3(a)] [28].

The $[Cu(L)_2]$ complex has UV-Vis absorption bands at 262, 378, and 397 nm [Figure 3]. A $[Cu(L)_2]$ altered the ligand's electronic spectra at 311 and 352 nm. L-bound Cu (II) ions. Peaks were attributed to π→π* transition at 262 nm and n→π* transition at 378 nm. The transitions are caused by azomethine nitrogen's lone electrons and antibonding p orbital. L-to-metal charge transfer in the compound's absorption band at 397 nm is seen in Figure 3. Based on the UV spectral data and magnetic moment value, it is conceivable that the $[Cu(L)_2]$ has a tetrahedral structure [Figure 3(b)].

Figure 3 shows three UV-Vis absorption bands at 260, 362, and 400 nm for $[Co(L)_2]$. The ligand's electronic spectra changed at 311 and 352 nm due to the $[Co(L)_2]$. L binding to Co (II) ions was shown. Peaks at 260 and 362 nm were assigned to the π→π* and n→π* transitions, respectively. The transitions are induced by azomethine nitrogen's lone electron pair and antibonding p orbital. The L transfers charge to the metal in the molecule's absorption band at 400 nm, as seen in Figure 3. Based on magnetic moment and UV spectral measurements, the $[Co(L)_2]$ may be tetrahedral [Figure 3(c)].

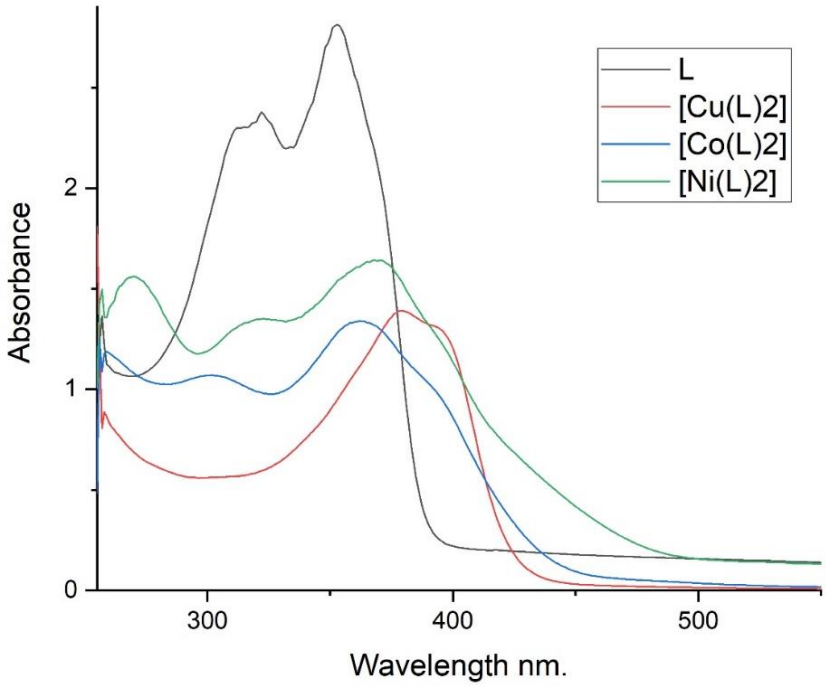

Figure 3. UV-Vis Spectra of L & Its Metal Complexes

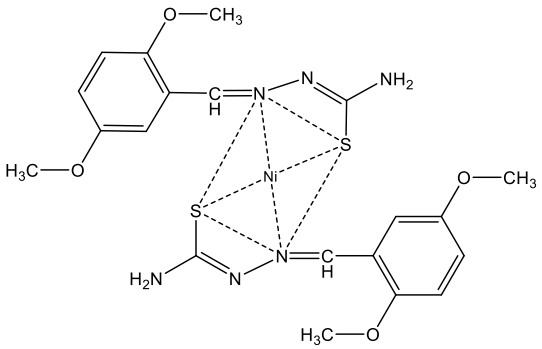

Figure 3(a). Probable square-planar geometry of $[NiC_{20}H_{24}O_4N_6S_2]$ complex

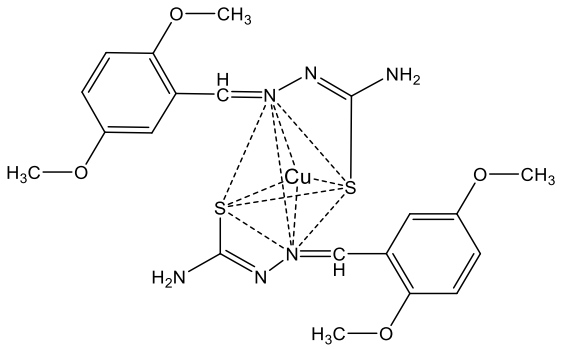

Figure 3(b). Probable tetrahedral geometry of $[CuC_{20}H_{24}O_4N_6S_2]$ complex

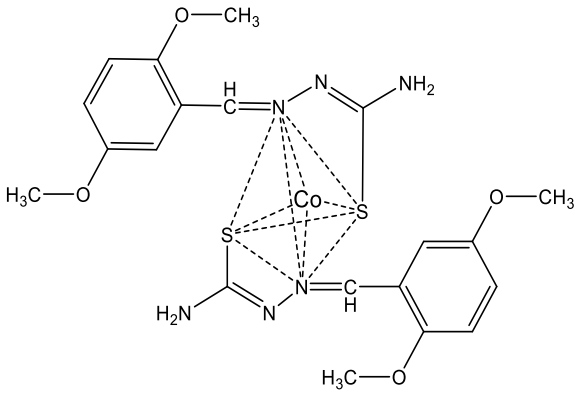

Figure 3(c). Probable tetrahedral geometry of $[CoC_{20}H_{24}O_4N_6S_2]$ complex

3.4. ESI-Mass Spectra

The obtained m/z values are similar to the formula weight of the studied compounds (Figure 4). This similarity supports the proposed structure of the synthesized compounds.

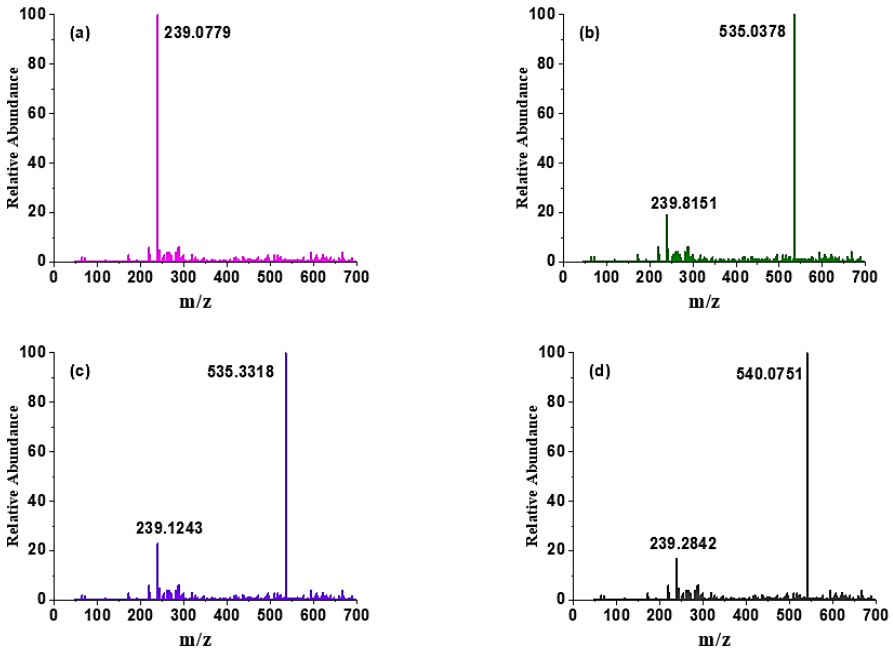

Figure 4. ESI-Mass Spectra for (a) Ligand, L (b) $[Ni(L)_2]$ (c) $[Co(L)_2]$ and (d) $[Cu(L)_2]$

3.5. Microbiological evaluation

L and its complexes (as shown in Table 4) were evaluated for their biological activity in conjunction with metal salts and standards. This evaluation was conducted using the filter paper disc technique against two gram-positive bacteria (*B. cereus* and *S. aureus*) and two gram-negative bacteria (*E. coli* and *P. aeruginosa*). Kanamycin-30 was employed as the benchmark against the corresponding microorganisms. The control was treated with DMSO. The antibacterial activity was assessed by measuring the diameter of the zone of inhibition produced around the wells in the plates. The Schiff bases examined in this investigation showed either lower or comparable activity against the microorganisms. The results of the antibacterial activity of various samples against pathogenic bacteria are shown in Figure 5 and Table 4. The unbound L and other complexes were less effective against E. Coli than the $[Ni(L)_2]$. According to Overtone's notion and Tweedy's chelation hypothesis, metal complexes are more effective against bacteria than unbound ligands [29].

Table 4. Electronic spectrum data and magnetic moments for L and its metal complexes.

Symbol of Compounds	Empirical formula	λ_{max} nm	μ_{eff} B.M	Assignment
L	$C_{20}H_{24}O_4N_6S_2$	311 352	---	π→π* n→π* C.T (L→M)
$[Ni(L)_2]$	$NiC_{20}H_{24}O_4N_6S_2$	268 321 370	Diamagnetic	π→π* n→π* C.T (L→M)
$[Co(L)_2]$	$CoC_{20}H_{24}O_4N_6S_2$	260 362 400	3.87	π→π* n→π* C.T (L→M)
$[Cu(L)_2]$	$CuC_{20}H_{24}O_4N_6S_2$	262 378 397	1.74	π→π* n→π* C.T (L→M)

Table 5. Antibacterial activities (zone of inhibition in mm) of samples against pathogens.

Samples	*P. aeruginosa*	*E. coli*	*B. cereus*	*S. aureus*
Kanamycin-30	27	24	25	26
L	10	8	8	9
$[Cu(L)_2]$	9	7	---	8
$[Ni(L)_2]$	10	13	7	7
$[Co(L)_2]$	6	7	---	---

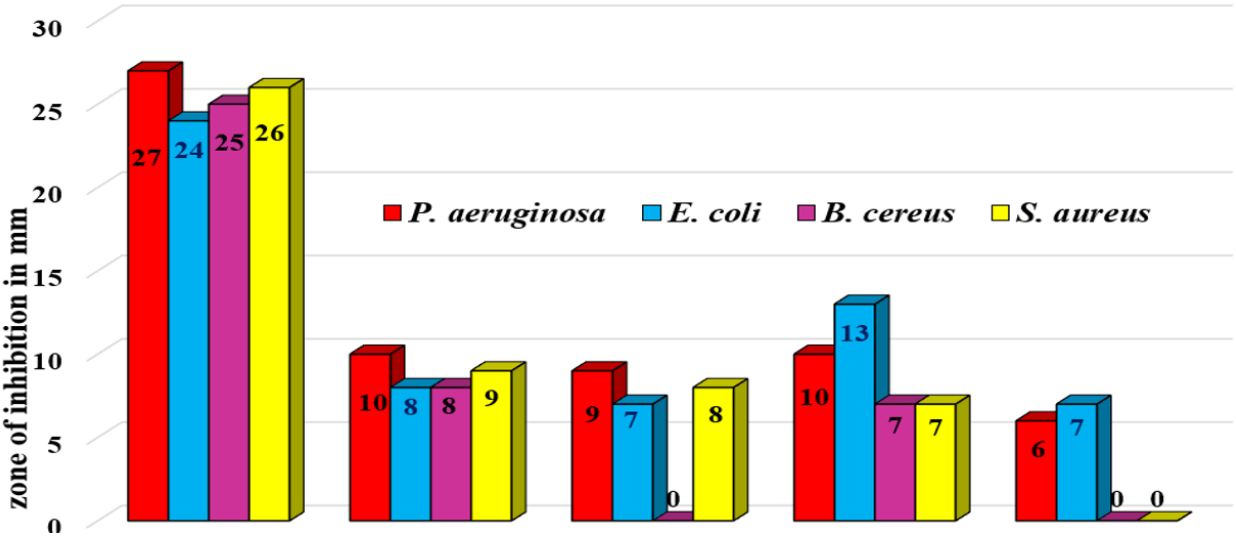

Figure 5. Zone of inhibition of samples & standard against *P. aeruginosa, E. coli, S. aureus* and *B. cereus*

3.6. Cytotoxicity evaluation

The synthesized Schiff base L and its metal complexes exhibit substantial activity in the brine shrimp lethality test, as shown in Table 5 and Figure 6. The current investigation demonstrated a direct correlation between the amounts of chemicals and the level of lethality [30]. The highest fatality rates were seen at the concentration of 100 ug/mL, while the lowest mortality rates were observed at the concentration of 6.25. The brine shrimp lethality test revealed that each synthesized compound exhibited positive findings, indicating that they possessed biological activity. The L and its metal complexes included in this group of materials exhibited a lower level of cytotoxicity, as evidenced by the LC_{50} values of 36.93 µg/mL, 43.16 µg/mL, 41.40 µg/mL, and 45.99 µg/mL, respectively, in comparison to the conventional vincristine sulfate, which had an LC_{50} value of 12.09 µg/mL.

Table 6. Brine Shrimp Lethality Bioassay.

Sample	Conc. Of the Sample (µg/ml)	Log conc. (µg/ml)	Number of nauplii used	Number of nauplii survived (After 24h)	Percentage of mortality	Probit value	LC_{50} Value (µg/ml)
Standard (vincristine sulfate)	6.25	0.7959	30	23	23	4.26	12.09
	12.5	1.0969	30	14	57	5.18	
	25	1.3979	30	10	67	5.44	
	50	1.6990	30	5	83	5.95	
	100	2.0000	30	0	100	8.95	
L	6.25	0.7959	15	13	13.33	3.87	36.93
	12.5	1.0969	15	13	13.33	3.87	
	25	1.3979	15	13	13.33	3.87	
	50	1.6990	15	3	80	5.84	
	100	2.0000	15	0	100	8.95	
$[Cu(L)_2]$	6.25	0.7959	15	13	13.33	3.87	43.16
	12.5	1.0969	15	13	13.33	3.87	
	25	1.3979	15	13	13.33	3.87	
	50	1.6990	15	6	60	5.25	
	100	2.0000	15	0	100	8.95	
$[Ni(L)_2]$	6.25	0.7959	14	12	14.28	3.92	41.40
	12.5	1.0969	14	12	14.28	3.92	
	25	1.3979	14	11	21.42	4.19	
	50	1.6990	14	6	57.14	5.18	
	100	2.0000	14	1	92.85	6.41	
$[Co(L)_2]$	6.25	0.7959	15	13	13.33	3.87	45.99
	12.5	1.0969	15	13	13.33	3.87	
	25	1.3979	15	13	13.33	3.87	
	50	1.6990	15	7	53.33	5.08	
	100	2.0000	15	0	100	8.95	

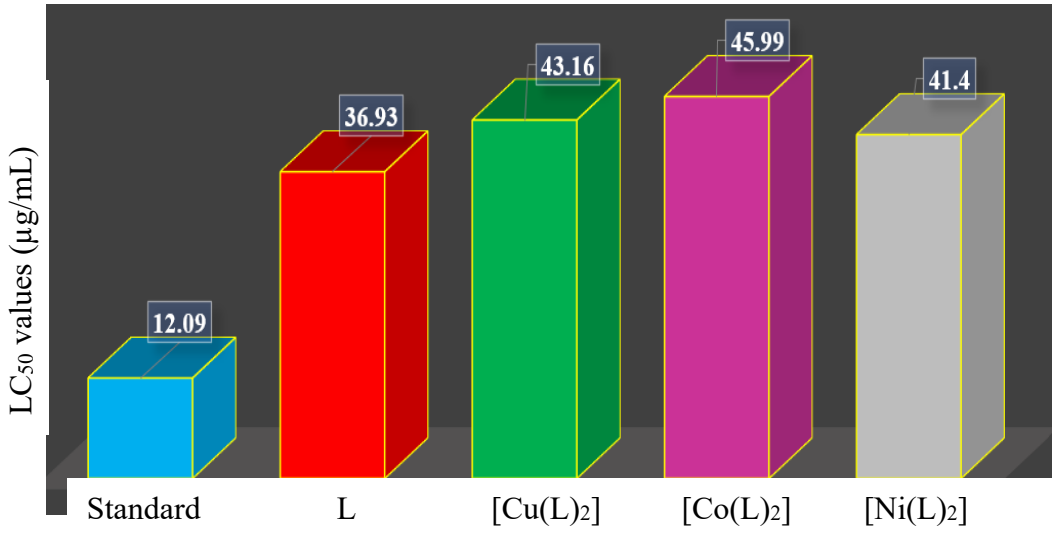

Figure 6. LC_{50} values of Sample & Standard

4. Conclusion

The Schiff base ligand 2-(2,5-dimethoxybenzylidene) hydrazine-1-carbothioamide and its mononuclear $[Ni(L)_2]$, $[Cu(L)_2]$, $[Co(L)_2]$ complexes were synthesized and well characterized. Among them, $[Ni(L)_2]$ was found to be square-planar, while the $[Cu(L)_2]$ and $[Co(L)_2]$ complexes are found to be tetrahedral in geometry. All compounds were preferentially active against brine shrimp nauplii, representing an intriguing cytotoxicity pattern observed compared to standard vincristine sulfate. Among them, the L showed a better LC_{50} value of 36.93 µg/mL than the others. However, more mechanisms of action and in vivo investigations are necessary to evaluate the action of these compounds in vivo to have a better knowledge of their activities within the cell. The antibacterial efficacy of compounds L and its $[Ni(L)_2]$, $[Co(L)_2]$, $[Cu(L)_2]$ complexes was assessed using the disc diffusion method against four different microorganisms. Out of the tested substances, the $[Ni(L)_2]$ showed a higher zone of inhibition (13 mm) against E. coli than other compounds.

Acknowledgment

The authors would like to thank the Chairman of the Department of Chemistry, University of Rajshahi, Bangladesh, for providing lab facilities.

Conflict of interest

The authors declare that they have no known competing interests that could influence the work reported in this paper.

References

1. N.A. Mazlan, T.B.S. Ravoof, E.R. Tiekink, M.I.M. Tahir, A. Veerakumarasivam, K.A. Crouse, Mixed-ligand metal complexes containing an ONS Schiff base and imidazole/benzimidazole ligands: Synthesis, characterization, crystallography and biological activity, Transition Metal Chemistry, **2014**, 39, 633-639.
2. Y.Han, Y. Sun, A. Abdukader, B. Liu, D. Wang, PhI-catalyzed intramolecular oxidative coupling toward Synthesis of 2-amino-1, 3, 4-thiadizoles, Catalysis Letters, **2018**, 148, 3486-3491.
3. A.D. Khalaji, G., Grivani, S.J. Akerdi, K. Gotoh, H. Ishida, H. Mighani, Synthesis, spectroscopic characterization, crystal structures, and theoretical studies of (E)-2-(2, 4-dimethoxybenzylidene) thiosemicarbazone and (E)-2-(2, 5-dimethoxybenzylidene) thiosemicarbazone, Structural Chemistry, **2010**, 21, 995-1003.
4. K. Jayanthi, R.P. Meena, K. Chithra, S. Kannan, W. Shanthi, R. Saravanan, M. Suresh, D. Satheesh, Synthesis and microbial evaluation of copper (II) complexes of Schiff base ligand derived from 3-methoxysalicylaldehyde with semicarbazide and thiosemicarbazide, Journal of Pharmaceutical, Chemical and Biological Sciences, **2017**, 5, 205-215.
5. A. Singh, P. Barman, Recent advances in Schiff base ruthenium metal complexes: Synthesis and applications, Topics in Current Chemistry, **2021**, 379, 1-71.
6. K. Ajay, Studies and Synthesis of new drugs formed with fluoroquinolones and metal ions, Int. J. of Life Sciences, **2018**, 6, 446-452.
7. A.A. Ali, H. Nimir, C. Aktas, V. Huch, U. Rauch, K.H. Schäfer, M. Veith, Organoplatinum (II) complexes with 2-acetylthiophene thiosemicarbazone: synthesis, characterization, crystal structures, and in vitro antitumor activity, Organometallics, **2012**, 31, 2256-2262
8. L.M. Aroua, S.K. Alhag, L.A. Al-Shuraym, S. Messaoudi, J.A. Mahyoub, M.Y. Alfaifi, W.M. Al-Otaibi, Synthesis and characterization of

different complexes derived from Schiff base and evaluation as a potential anticancer, antimicrobial, and insecticide agent, Saudi Journal of Biological Sciences, **2023**. 30, 103598.
9. A.J.M. Al-Karawi, Synthesis and characterization of a new N 2 S 2 Schiff base ligand and its complexes with nickel (II), copper (II) and cadmium (II) including the kinetics of complex formation, Transition metal chemistry, **2009**, 34, 891-897.
10. H. Wang, P. Zhao, D. Shao, J. Zhang, Y. Zhu, Synthesis, characterization and spectra studies on Zn (II) and Cu (II) complexes with thiocarbamide ligand containing Schiff base group, Structural Chemistry, **2009**, 20, 995-1003.
11. J. Joseph, N.L. Mary, R. Sidambaram, Synthesis, characterization, and antibacterial activity of the Schiff bases derived from thiosemicarbazide, Salicylaldehyde, 5-bromosalicylaldehyde and their copper (II) and nickel (II) complexes, Synthesis and Reactivity in Inorganic, Metal-Organic, and Nano-Metal Chemistry, **2010**, 40, 930-933.
12. F.S. Tokalı, P. Taslimi, H. Usanmaz, M. Karaman, K. Şendil, Synthesis, characterization, biological activity and molecular docking studies of novel Schiff bases derived from thiosemicarbazide: Biochemical and computational approach, Journal of Molecular Structure, **2021**, 1231, 129666.
13. H. Wang, A.M.S. Hossain, Q. Zhang, J. Wu, Y. Tian, Synthesis, crystal structures and third-order nonlinear optical properties of 4-formylpyridine Schiff base of thiosemicarbazide, and its dinuclear copper (I) and silver (I) complexes, Inorganica Chimica Acta, **2014**, 414, 153-159.
14. N.N. Ishak, J. Jamsari, A.Z. Ismail, M.I. Tahir, E.R. Tiekink, A. Veerakumarasivam, T.B. Ravoof, Synthesis, characterisation and biological studies of mixed-ligand nickel (II) complexes containing imidazole derivatives and thiosemicarbazide Schiff bases, Journal of Molecular Structure, **2019**, 1198, 126888.
15. A.A. Al-Amiery, Y.K. Al-Majedy, H.H. Ibrahim, A.A. Al-Tamimi, Antioxidant, antimicrobial, and theoretical studies of the thiosemicarbazone derivative Schiff base 2-(2-imino-1-methylimidazolidin-4-ylidene) hydrazinecarbothioamide (IMHC), Organic and medicinal chemistry letters, **2012**, 2, 1-7.
16. M. Mohammadikish, M. Masteri-Farahani, S. Mahdavi, Immobilized molybdenum–thiosemicarbazide Schiff base complex on the surface of magnetite nanoparticles as a new nanocatalyst for the epoxidation of olefins, Journal of magnetism and magnetic materials, **2014**, 354, 317-323.
17. I. Babahan, F. Eyduran, E.P. Coban, N. Orhan, D. Kazar, H. Biyik, Spectroscopic and biological approach of Ni (II), Cu (II) and Co (II) complexes of 4-methoxy/ethoxybenzaldehyde thiosemicarbazone glyoxime, Spectrochimica Acta Part A: Molecular and Biomolecular Spectroscopy, **2014**, 121, 205-215.
18. D. Shobana, S. Sudha, D. Ramarajan, N. Ristivojević, A. Rakić, D. Dimić, Structural, spectroscopic (IR, Raman, and NMR), quantum chemical, and molecular docking analysis of (E)-2-(2, 5-dimethoxybenzylidene) hydrazinecarbothioamide and its dimers, Journal of Molecular Structure, **2022**, 1247, 131277.
19. P.S. Zhao, H.Y. Wang, J. Song, L.D. Lu, Synthesis, structures, and property studies on Zn (II), Ni (II), and Cu (II) complexes with a Schiff base ligand containing thiocarbamide group, Structural Chemistry, **2010**, 21, 977-987.
20. S. Feizpour, S.A. Hosseini-Yazdi, E. Safarzadeh, B. Baradaran, M. Dusek, M. Poupon, A novel water-soluble thiosemicarbazone Schiff base ligand and its complexes as potential anticancer agents and cellular fluorescence imaging, JBIC Journal of Biological Inorganic Chemistry, **2023**, 1-16.
21. M.N. Al-Jibouri, S.M. Hasun, Synthesis and characterization of manganese (II), cobalt (II), nickel (II), copper (II) and zinc (II) complexes with new Schiff base derived from 6, 7-dimethyl-quinoxaline-2, 3 (1H, 4H)-dione and thiosemicarbazide, European Journal of Chemistry, **2015**, 6, 44-47.
22. L.F. Chu, Y. Shi, D.F. Xu, H. Yu, J.R. Lin, Q.Z. He, Synthesis and biological studies of some lanthanide complexes of schiff base, Synthesis and Reactivity in Inorganic, Metal-Organic, and Nano-Metal Chemistry, **2015**, 45, 1617-1626.
23. K.S. Abou-Melha, Octahedral Co (II) and Ni (II) complexes of Schiff bases, semicarbazone and thiosemicarbazone, Synthesis, biological, spectral, and thermal studies, Journal of Coordination Chemistry, **2008**, 61, 2053-2067.
24. O.K. Nehar, R. Mahboub, S. Louhibi, T. Roisnel, M. Aissaoui, New thiosemicarbazone Schiff base ligands: Synthesis, characterization, catecholase study and hemolytic activity, Journal of Molecular Structure, **2020**, 1204, 127566.
25. A.J.M Al-Karawi, Synthesis and characterization of a new N 2 S 2 Schiff base ligand and its complexes with nickel (II), copper (II) and cadmium (II) including the kinetics of complex formation, Transition metal chemistry, **2009**, 34, 891-897.
26. S.H. Gordon, A. Mohamed, R.E. Harry-O'Kuru, S.H. Imam, A chemometric method for correcting Fourier transform infrared spectra of biomaterials for interference from water in KBr discs, Applied spectroscopy, **2010**, 4, 448-457.
27. A.A. Al-Amiery, Synthesis and antioxidant, antimicrobial evaluation, DFT studies of novel metal complexes derivate from Schiff base, Research on Chemical Intermediates, **2012**, 3, 745-759.

28. A. Çukurovali, I. Yilmaz, H. Özmen, M. Ahmedzade, Cobalt (II), copper (II), nickel (II) and zinc (II) complexes of two novel Schiff base ligands and their antimicrobial activity, Transition metal chemistry, **2002**, 27, 171-176.
29. F.K. Camellia, M. Ashrafuzzaman, M.N. Islam, L.A. Banu, M.K. Zahan, Synthesis, characterization, antibacterial and antioxidant studies of isoniazid-based Schiff base ligands and their metal complexes. Asian Journal of Applied Chemistry Research, **2022**, 11(3), 8-23.
30. S. Ramachandran, M. Vamsikrishna, K.V. Gowthami, B. Heera, M.D. Dhanaraju, Assessment of cytotoxic activity of Agave cantula using brine shrimp (Artemia salina) lethality bioassay, Asian J Sci Res, **2011**, 4, 90-104.